The paper was published in the proceedings of the 7th International Conference on Earthquake Geotechnical Engineering and was edited by Francesco Silvestri, Nicola Moraci and Susanna Antonielli. The conference was held in Rome, Italy, 17 – 20 June 2019.

Earthquake Geotechnical Engineering for Protection and Development of Environment and Constructions – Silvestri & Moraci (Eds)
© 2019 Associazione Geotecnica Italiana, Rome, Italy, ISBN 978-0-367-14328-2

Epistemic uncertainty quantification for 1D ground response analysis using fully nonlinear models

V. Alves Fernandes
Electricité de France/R&D, Palaiseau, France SEISM Institute, France

S. Montoya-Noguera
Universidad EAFIT, Medellin, Colombia

E. Foerster
CEA/DEN/EMSI, Gif-sur-Yvette, France
SEISM Institute, France

F. Lopez-Caballero
Laboratoire MSS-Mat CNRS UMR 8579, CentraleSupélec, Université Paris Saclay, FranceSEISM Institute, France

M. Jacquet & D. Vandeputte
Electricité de France/DI/TEGG, Aix-en-Provence, France

ABSTRACT: The validation phase of the PRENOLIN benchmark (Régnier & al., 2018) allowed assessing epistemic uncertainties for 1D ground response analysis (1D GRA) for a large class of modeling strategies and numerical procedures. In this work, the results of three teams using the ECP/Hujeux model are further analyzed for the Sendai site. Although being the simplest site configuration (shallow soil deposit of gravel and sandy soil), it presented difficulties inherent of current 1D GRA. Therefore, the main objective of this work is to pinpoint the principal sources epistemic uncertainty for calibration of this type of model and how they can affect the different quantities of interest for 1D GRA.

1 INTRODUCTION

Quantifying epistemic uncertainties on site effects estimation for seismic hazard assessment based on numerical simulations requires to correctly estimate the validity domains of different modeling strategies. These strategies are related, for example, to the geometric characteristics of the site, the analysis type (effective or total stress analysis), the boundary conditions, and the material rheology. Very often, 1D wave propagation is considered, as it simplifies the associated numerical model to account solely for the stratigraphic effects while a vertical plane shear-wave is used as input. For this particular case, epistemic uncertainties arise not only from the 1D simplification but also from model‘s hypotheses related to the material rheology, both from the capacity of the chosen rheology model to reproduce the important physical features associated to site effects and from the usual available data that is used for the model calibration. In this sense, different models are available to account for soil nonlinearity. These can be divided into two classes: models that follow cyclic shear stress-strain relationships with loading and unloading rules, and fully nonlinear models (or advanced constitutive models) which define yield surfaces, hardening laws and flow rules from the rheological behavior of the material.

PRENOLIN benchmark (https://prenolin.org) focused on epistemic uncertainty quantification for nonlinear 1D ground response analysis (1D GRA). During the validation phase

(Régnier & al., 2018), participants had at hand usual available data for 1D GRA (estimated Vs and shear strength profiles and nonlinear curves, i.e. G/G_{max}-$\lambda$and D-λ), but this information is not enough for calibrating rheological based models. Therefore, additional hypotheses (such as initial relative density and material dilatancy) had to be made for model calibration, which may lead to epistemic uncertainties for research groups using the same family of models but considering different calibration procedures.

Therefore, the main objective of this work is to analyze how calibration procedures can affect the epistemic uncertainties on nonlinear 1D GRA when considering nonlinear elastoplastic constitutive models (i.e. user-code variability). The analysis is performed on the PRENOLIN benchmark results for Sendai site using the Hujeux/ECP model family Aubry1982, which are elastoplastic multimechanism models used to simulate soil behavior for both monotonic and cyclic loading. Three research groups used this models family in the PRENOLIN benchmark and a detailed analysis of their results is performed based on the hypotheses chosen by each group for the model calibration. The three teams collaborating in this work are:

- EDF team, using the code_aster software (team S-0)
- CentraleSupélec (CS) team, using Gefdyn software (team N-0)
- CEA team, using CyberQuake software (team D-0)

2 CONSIDERED SITE AND SIGNALS

The selected site for the presented analysis is the first of the two considered sites for the validation phase of the PRENOLIN benchmark, that is, Sendai site from the Port and Airport Research Institute (PARI). It is a shallow deposit composed of 3 layers: a thin gravel (down to GL -1m) and a sandy soil layer (down to GL-7m), followed by a Pliocene, Geba Formation, forming the northern and eastern hills and consist of gravel stone, sandstone, tuff, tuffaceous siltstone, and lignite (Régnier & al., 2018). The downhole sensor is positioned at GL-10.4m. The site presented a predominant resonant frequency for weak motions around 8 Hz, which can be viewed as a rather rigid site.

The numerical simulations performed considered nonlinear characteristics only for the first two layers. The elastic soil column properties and considered nonlinear characteristics are given on Table 1 and Figure 1. Two approaches for obtaining nonlinear properties were investigated: either standard curves available from the literature (Darendelli, 2001) (SC1) or laboratory test results from cyclic triaxial tests (SC2). SC1 presents higher nonlinear behavior than SC2, i.e. the Darendelli (2001) curves present more shear modulus reduction and more damping for the same shear strains than those observed on the laboratory tests.

The considered input motions are the same used on the PRENOLIN benchmark. They were selected in order to obtain three acceleration levels at the downhole sensor (lower than $0.1m/s^2$, between $0.2m/s^2$ and $0.3m/s^2$, higher than $0.6m/s^2$), and different frequency content. Detailed information of signals can be found on Régnier & al. (2018).

Table 1. Linear and nonlinear properties of Sendai site.

Layer		Elastic Properties				Nonlinear properties		
#	GL [m]	Vs [m/s^2]	Vp [m/s^2]	ρ [kg/m^3]	Qs	SC1	SC2	τ_{max} [kPa]
1	0-1	120	610	1850	25	1	1	5
2	1-2	170	870	1850	25	2	1	5-11
3	2-3	200	1040	1850	7.14	3	1	11-16
4	3-4	230	1180	1890	7.14	4	2	16-21
5	4-5	260	1300	1890	7.14	5	2	21-27
6	5-6	280	1420	1890	7.14	6	2	27-32
7	6-7	300	1530	1890	7.14	7	2	32-39
8	7-10.4	550	2800	2480	50	-	-	-

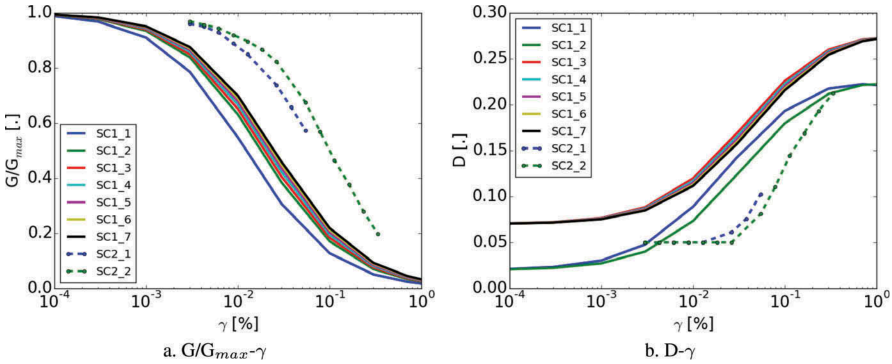

Figure 1. Reference SC1 and SC2 curves for Sendai site.

Most of the input motions considered during the benchmark for the Sendai site do not exhibited linear polarization. Therefore, considering 1D wave propagation for these signals is a strong hypothesis, as the input motions do not present the characteristics necessary for this hypothesis to hold. A more realistic wave field would require a mixture of body and surface waves, which could be prescribed on a 2D/3D model only if the full wave field (displacements plus rotations) were available. Nonetheless, calculations are performed with this hypothesis as it is the current practice for assessing ground response analysis. Input motions are imposed at the base of the soil column on a rigid-base approach, as signals are from borehole sensors (Bonilla & al., 2002).

3 OVERVIEW OF HUJEUX/ECP MODEL FAMILY AND CALIBRATION PROCEDURE

The ECP/Hujeux model assumes effective stress approach (although it can be used on a total stress fashion by adapting the mass density of the soil (Montoya-Noguera & Lopez-Caballero, 2018)) and it is based on a Coulomb type failure criterion and critical state concept (Roscoe & al., 1958). The fully 3D formulation of the model considers 3 plane-strain deviatoric plastic mechanisms and one isotropic, coupled by plastic volumetric strain. Both monotonic and cyclic behavior of soils are modeled by considering isotropic and kinematic hardening, the last one based on the state variables at the last load reversal. This version of the model was used by both CS (Gefdyn software) and EDF (code_aster software) teams.

In the 1D version of the Hujeux model implemented in CyberQuake (Foerster & Modaressi, 2007) and used by the CEA team, the formulation is expressed in the principal stress space, considering only one isotropic and one plane-strain deviatoric mechanisms. In addition, contrary to the full 3D formulation, there is no dependency of the shear and bulk moduli with respect to the mean effective stress. Hence, a fine discretization of the soil profile layers is to be implemented to introduce this dependency explicitly. Finally, another difference existing between the 1D and 3D formulations, is related to the damping at high shear strain levels: in the 1D version, the user provides a “degradation-type” curve for the plastic tangent modulus with respect to the shear strains, hence leading to limiting the over-damping usually observed at high strain levels.

In the following, the main aspects for the calibration procedure followed by the different teams are described. The data given by the benchmark was the proposed G/G_{max} and damping curves (SC1 or SC2) as well as the maximum shear stress at each layer. One difficulty faced on calibrating the ECP/Hujeux model was to define the material state at site, i.e. wherever the sandy soil presents dense or loose state at the confining pressure at site. Mostly of the considered models used in the benchmark do not accounted for critical state concept, such as the Iwan model (Iwan, 1967, Mróz, 1967), used by different research teams. In this case, the maximum shear stress can be used for calibrating the model as it implicitly supposes a loose behavior.

Another important point on the calibration is the influence of mean stress on the deviatoric material behavior. Indeed, the ECP/Hujeux model takes into account the influence of mean stress on the G/G_{max} and damping curves. Therefore, the calibration procedure must consider the expected mean stress at the different depths of the soil column and adapt the model parameters for the prescribed G/G_{max} and damping curves. In order to better control this point and following the instructions given during the benchmark, teams considered one layer at every meter and for each layer set the n_{el} = 0, i.e. the shear and bulk moduli no longer depend on the mean stress. Particularly for the Hujeux/ECP model, the calibration of the damping curves is usually difficult as it under estimates damping at low strains and overestimate it at higher strains. At strains lower than 0.01%, a small amount of damping, usually less than 0.1% is added to the model by the numerical algorithm. Moreover, the calibration of fully nonlinear models based solely on the deviatoric behavior curves cannot be fully conducted without assessing the expected volumetric behavior, specially in the case where effective stress is considered.

Finally, during the different iterations of the validation phase accent was given for predictions of EW component for the Sendai site, as it was found to present less discrepancy than the NS component (Régnier & al., 2018). Although blind predictions were performed during the first iteration, results presented here were obtained after the second iteration, for which surface motions were provided.

3.1 *Calibration hypothesis for the different teams*

The EDF team considered the sandy soil on the first 7 m as a standard sand with a friction angle at critical state of 31° and a dense state with low plastic compressibility. Values of τ_{max} at each layer were calibrated according to the expected strain level in the material. The EDF team considered maximum values of 5.10^{-3} for calibrating maximum shear stress (Figure 2). This value is based on the expected maximum shear strains based on Linear Equivalent calculations for TS-1-S. Small-strain damping is implemented by considering an equivalent Rayleigh damping on the frequency range 5 to 22 Hz. Numerical damping is also considered by using an HHT numerical scheme (Hilber & al., 1977) with α=-0.05, which leads to 1% damping at 13 Hz.

The CentraleSupélec team modeled the deposit as two layers of sandy soil following the first iteration indications of the PRENOLIN team. The first layer to a depth of 3 m and the second one to a depth of 7 m. The friction angle at critical state for the upper layer was set to 32° and for the lower one to 30°. Most of the model parameters were considered for a standard sand, at a medium dense state with medium plastic compressibility. To adjust the model for a constant shear and Bulk moduli at every meter as prescribed by the PRENOLIN team, the elastic behavior was set to be independent of the mean stress. Numerical damping of 1% is added in the Newmark integration scheme to assure unconditional stability with optimal high-frequency dissipation and minimum low-frequency impact.

The CEA team modeled the soil profile as two layers of sandy soil, each layer being subdivided by sub layers of 1m depth each. Following the indications of the PRENOLIN team, the friction angle at critical state was set to 44° for both layers. Model parameters were calibrated considering a medium dense state with medium plastic compressibility. Numerical damping of 1% has been added in the Newmark integration scheme.

3.2 *Comparison of calibration procedure on cyclic shear test results*

Figure 2 presents a comparison of cyclic shear test result for SC1 parameters for material #4. EDF calibration procedure lead to a lower τ_{max} value than CS, although differences are most visible starting from 0.5% shear strain. On the other hand, the calibration of CEA team lead to higher shear stress values for all imposed shear strains, as a consequence of the higher friction angle considered compared to both EDF and CS teams.

4 COMPARATIVE RESULTS FOR WEAK MOTION (TS-9-S)

Results on the weakest motion are first analyzed in order to evaluate the impact of modeling hypothesis on the numerical results obtained by each team, before considering soil

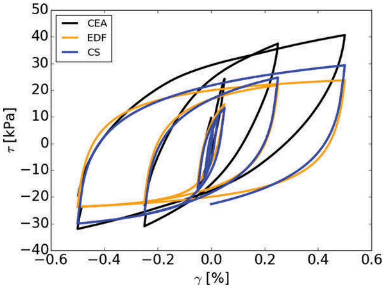

Figure 2. Results of standard cyclic shear test used for calibrating G/G_{max} and damping curves, material #4.

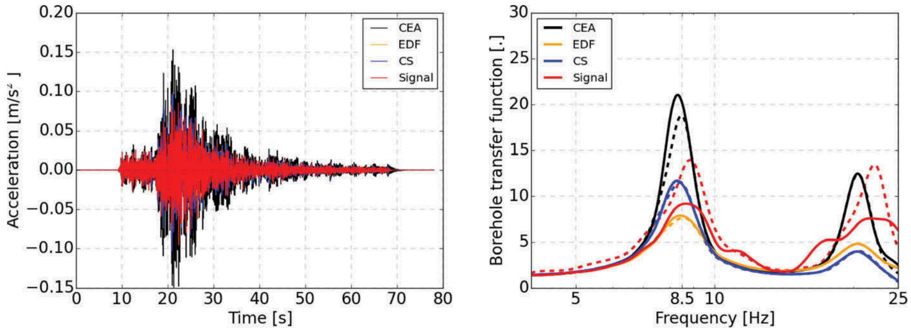

a. EW component

b. Borehole transfer function

Figure 3. Results for weakest input motion (TS-9-S) with soil column 1 (SC1): (a) Surface acceleration time series for EW component and (b) borehole transfer function for EW and NS components (solid line and dashed line, respectively).

nonlinearity. Pseudo-accelerations are calculated with 5% damping and borehole transfer functions are obtained from filtered FFT of the time-histories by applying Konno-Omachi filtering (Konno & Ohmachi, 1998) with b=40.

For the weak signal, SC1 and SC2 are strongly similar, as shear strains are very small on the soil column. Therefore, results of time histories and pseudo-acceleration are presented for SC1 only (Figure 3). The predicted numerical results are mainly dependent on the soil column elastic parameters (Vs and material damping) and numerical damping. A large variability for weak motions is observed among the three teams, which is mainly attributed on damping characteristics implemented on each numerical procedure.

Moreover, the borehole amplification for NS component is higher than EW component (Figure 3b), which cannot be obtained on the 1D-1C modeling approach. Therefore, the amplification of the predominant resonant pic for both components cannot be correctly predicted for the same input parameters by any team. This variability is mainly attributable to wave passage effects and should be accounted as epistemic uncertainty when dealing with 1D-1C modeling.

5 COMPARATIVE RESULTS FOR STRONG MOTION (TS-1-S)

The differences on the implementation of small strain damping characteristics by each team present a smaller impact on the predicted free-field time-histories for strong input motion, as the material nonlinearity becomes the major source of energy dissipation in the small to medium frequency range. Indeed, Figure 4 shows the borehole transfer functions for SC1 and SC2 nonlinear properties hypotheses. As discussed by Régnier & al. (2018), SC1 nonlinear properties provided better results for the Sendai site, as SC2 lead to an overestimated response of the soil column, i.e.

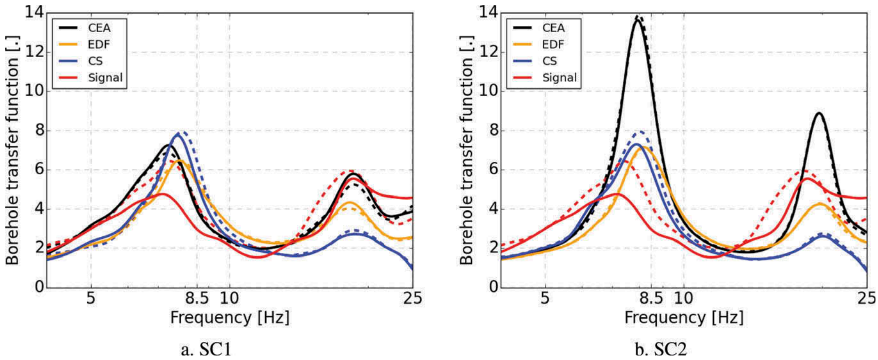

Figure 4. Borehole transfer function for TS-1-S input motion for EW and NS components (solid line and dashed line, respectively): (a) SC1 and (b) SC2.

higher amplitudes in acceleration and higher predominant frequency as a result of less damping and higher shear modulus, which in turn leads to a higher borehole transfer function. In the high frequency range, however, the differences in implemented damping strategies by each team are again observed, as the variability of the predicted borehole transfer function increases.

This strong motion also leads to higher NS component amplitude for the borehole transfer function than the EW component, as for the considered weak motion. However, this difference is not always as important for all the considered signals, although EW borehole transfer functions obtained is repeatedly slightly lower than NS component. All teams better predicted NS component, both in terms of predominant resonant frequency and amplitude.

The impact of soil non linearity on 1D ground response analysis can also be appreciated by considering the 1D Ratio of spectral response nonlinear to linear (1D RSR NL-L). The 1D RSR NL-L considered in this work is adapted from Régnier & al. (2016) and is obtained by simply dividing the surface/borehole frequency response modulus function of the considered signal by the soil column transfer function modulus under small strains conditions. Input motion 9 is used as representative for small strain condition.

Results presented on Figure 5 show that the amplification on small frequencies predicted by the numerical models with SC1 soil nonlinear properties varies in accordance with the variability observed between EW and NS components. Indeed, EDF and CS teams better predicted the nonlinearity on NS component (dashed line), whereas CEA team provided robust results for EW component (solid line) for a large frequency range, although predictions for the borehole transfer function of TS-9-S and TS-1-S were not in accordance for the EW component.

Differences on small frequency of the 1D RSR NL-L for measured EW and NS components are related to wave passage effects and non-vertical wave incidence, both for TS-1-S and

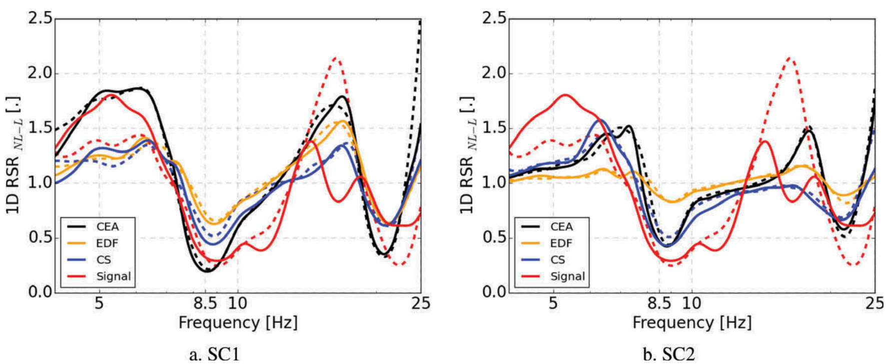

Figure 5. 1D Ratio of spectral response for TS-1-S input motion for SC1 (left-hand side) and SC2 (right-hand side) parameters. Full line: EW component; dashed line: NS component.

TS-9-S, which were already observed on the borehole transfer function. As expected, the 1D RSR NL-L is better modeled by SC1 than SC2 soil nonlinear properties.

6 COMPARISON OF ANDERSON'S CRITERIA

The goodness-of-fit (gof) of the considered EDPs is calculated following Anderson's criteria (Anderson, 2004). These are the following:

1. Peak ground acceleration (PGA),
2. Cumulative absolute velocity (CAV) (Reed & al., 1988),
3. Relative significant duration (RSD) (Kempton & Stewart, 2006),
4. Cross-correlation of time signals (COR),
5. Fourier amplitude acceleration over 3 frequency bands: low-frequency range between 1-4Hz (FA1), frequency range between f_0 -0.5 and f_0 +0.5 Hz with f_0=9Hz the elastic resonant frequency of the site (FA2), between 0.05 and 25 Hz (FA3), where 25 Hz was the maximum target frequency for nonlinear computations.

Anderson's criteria results for SC1, EW component are shown on Figure 6 for all 9 signals considered in the benchmark. Results for most signals and components present at least a good fit (values higher than 6, which means a maximum difference of 70% between measurements and numerical values) and in some cases an excellent fit (values higher than 8, which means a maximum difference of 47% between measurements and numerical values). A good fit is obtained for the cross correlation (COR) for most input motions, which proved to be the most difficult parameter to fit, especially for input motions with higher amplitude.

Moreover, the significant differences exemplified on the previous section for the borehole transfer function for weak input motion 9 also impacts Anderson's criteria results, specially Fourier acceleration amplitude. Input motion TS-5-S also presented lower gof values, but in this cases Régnier & al. (2018) already argued that differences with this motion is associated with the input motion specificity. Therefore, the modeling strategies applied by the three considered teams based on the ECP/Hujeux numerical model for this simple yet pertinent study case lead to robust predictions of free-field acceleration for different borehole input motions.

7 CONCLUSIONS AND PERSPECTIVES

The PRENOLIN benchmark (https://prenolin.org) allowed different research and industrial teams to verify and test their numerical tools and methods for assessing 1D ground response analysis. Among the sites used for the validation phase, the Sendai site from the Port and Airport Research Institute (PARI) presented the simplest configuration (shallow soil deposit of

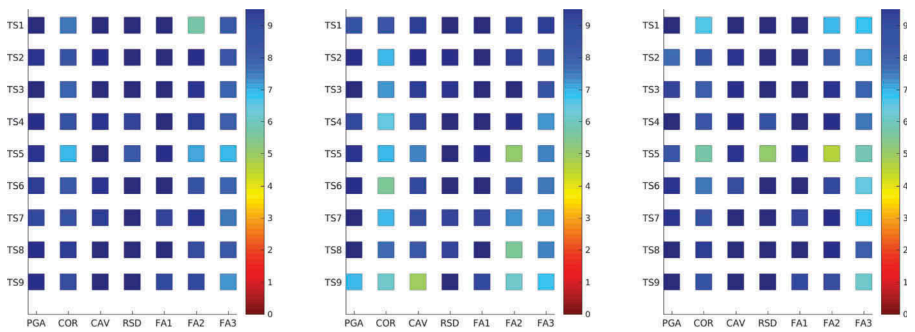

a. EDF

b. CEA

c. CS

Figure 6. Anderson's criteria for SC1 nonlinear properties, EW component.

gravel and sandy soil). Nonetheless, it presented difficulties inherent of current 1D GRA, such as: possible non vertical incidence, wave motion passage effects.

The three teams using Hujeux/ECP model successfully obtained the main features of the Sendai site response with SC1 soil properties. SC2 soil properties did not lead to sufficient nonlinear behavior, which is clearly pointed out by the 1D RSR NL-L results. Anderson‘s criteria showed that EW component was better captured than NS component for most signals, which was globally observed during the benchmark exercise (R´egnier & al., 2018).

The variability observed between different numerical results for weak motions is mainly attributable to small-strain damping implemented by the different teams, both material and numerical damping. For strong motions, the variability is mainly controlled by the nonlinear soil properties at low and medium frequencies, and by the numerical damping at high frequencies. Small code-to-code variability is observed between the three teams for strong motions for borehole transfer function using SC1 soil nonlinear properties. However, the role of soil nonlinearity in Sendai site response was differently modeled by the three teams, as the amplitude of elastic response presents a larger code-to-code variability. In this sense, it seems of most importance to correctly assess the amplitude of site small-strain response previously to conduct any nonlinear GRA model.

REFERENCES

Anderson, J. G. 2004. Quantitative measure of the goodness-of-fit of synthetic seismograms. In *Procceedings of the 13th World Conference on Earthquake Engineering, Vancouver, BC, Canada*, pp. Paper 243. Balkema.

Aubry, D., J.-C. Hujeux, F. Lassoudière, & Y. Meimon 1982. A double memory model with multiple mechanisms for cyclic soil behaviour. In *Int. Symp. Num. Mod. Geomech.*, pp. 3–13. Balkema.

Bonilla, L. F., J. H. Steidl, J.-C. Gariel, & R. J. Archuleta 2002. Borehole response studies at the Garner Valley Downhole Array, Southern California. *Bulletin of the Seismological Society of America 92*(8), 3165.

Darendeli, M. B. 2001. Development of a new family of normalized modulus reduction and material damping curves.

Foerster, E. & H. Modaressi 2007. Nonlinear numerical method for earthquake site response analysis ii — case studies. *Bulletin of Earthquake Engineering 5*(3), 325–345.

Hilber, H. M., T. J. R. Hughes, & R. L. Taylor 1977. Improved numerical dissipation for time integration algorithms in structural dynamics. *Earthquake Engineering & Structural Dynamics 5*(3), 283–292.

Iwan, W. D. 1967. On a class of models for the yeilding behavior of continuous and composite systems. *Journal of Applied Mechanics 89*(13), 612–617.

Kempton, J. J. & J. P. Stewart 2006. Prediction equations for significant duration of earthquake ground motions consideringsiteandnear-sourceeffects. *Earthquake Spectra 22*(4), 985–1013.

Konno, K. & T. Ohmachi 1998. Ground-motion characteristics estimated from spectral ratio between horizontal and vertical components of microtremor. *Bulletin of the Seismological Society of America 88*(1), 228.

Montoya-Noguera, S. & F. Lopez-Caballero 2018. Effect of coupling excess pore pressure and soil deformation on nonlinear SSI in liquefiable soil deposits. *Bulletin of Earthquake Engineering 16*(2), 681–705.

Mróz, Z. 1967. On the description of anisotropic work hardening. *Journal of Mechanics and Physics of Solids 15*(3), 163–175.

Reed, J. W., N. Anderson, N. C. Chokshi, R. P. Kennedy, W. J. Metevia, D. K. Ostrom, & J. D. Stevenson 1988. A criterion for determining exceedance of the operating basis earthquake. Technical report, Electrical Power Research Institute, Report No. EPRI NP-5930.

Régnier, J., L. F. Bonilla, P.-Y. Bard, E. Bertrand, F. Hollender, H. Kawase, D. Sicilia, & all 2016. International benchmark on numerical simulations for 1d, nonlinear site response (prenolin): Verification phase based on canonical casesinternational benchmark on numerical simulations for 1d, nonlinear site response (prenolin). *Bulletin of the Seismological Society of America 106*(5), 2112.

Régnier, J., L. F. Bonilla, P.-Y. Bard, E. Bertrand, F. Hollender, H. Kawase, D. Sicilia, & all 2018. Prenolin: International benchmark on 1d nonlinear siteresponse analysis validation phase exercisepreno-lin: International benchmark on 1d nonlinear siteresponse analysis validation phase exercise. *Bulletin of the Seismological Society of America 108*(2), 876.

Roscoe, K. H., A. N. Schofield, & C. P. Wroth 1958. On the yielding of soils. *Géotechnique 8*(1), 22–52.